RSC Advances

This is an *Accepted Manuscript*, which has been through the Royal Society of Chemistry peer review process and has been accepted for publication.

Accepted Manuscripts are published online shortly after acceptance, before technical editing, formatting and proof reading. Using this free service, authors can make their results available to the community, in citable form, before we publish the edited article. This *Accepted Manuscript* will be replaced by the edited, formatted and paginated article as soon as this is available.

You can find more information about *Accepted Manuscripts* in the **Information for Authors**.

Journal Name

Dynamic Article Links ▶

ARTICLE TYPE

Poly(ionic liquid) Janus Nanosheets towards Dye Degradation

Xuyang Ji[a,b], Qian Zhang[a], Xiaozhong Qu[b], Qian Wang[b], Xi-Ming Song*[a], Fuxin Liang*[b] and Zhenzhong Yang[b]
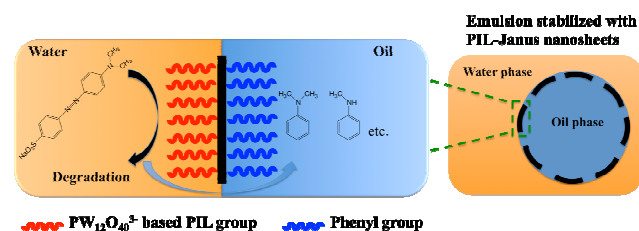
Polymeric ionic liquid (PIL) functionalized Janus nanosheets are synthesized by polymerization of ionic liquid monomer onto the ATRP agent modified side of the silica Janus nanosheets. $PW_{12}O_{40}^{3-}$ anion is introduced onto the PIL side 10 through anion exchange. The $PW_{12}O_{40}^{3-}$ based PIL Janus nanosheets at an emulsion interface exhibit excellent catalytic degradation of water soluble dyes for example methyl orange (MO).

Water pollution by organic dyes is becoming a concern. [1-2] 15 Among the dyes, water soluble azo based dyes are more difficult to treat by conventional methods. Some methods have been proposed including chemical oxidation, [3] adsorption [4] and biological catalytic degradation [5] to remove the azo dyes. Chemical oxidation is more welcomed due to its high degradation 20 efficiency. Selection of oxidants is key. Recently, highly redox active Keggin structured polyoxometalates (POMs) for example $H_3PW_{12}O_{40}$ have been reported. [6] POMs are required to support onto some matrices including silica particles and graphene. [7-8] The dyes are usually degraded into hydrophobic intermediate 25 products. [9] How to transfer the intermediate products becomes a key restricted step.

We have recently reported the synthesis of silica based Janus nanosheets and their functionalized derivatives including ionic liquid ones. [10-13] We conjecture that POMs based silica Janus 30 nanosheets will facilitate transferring the intermediate products during the oxidative degradation.

Scheme 1. $PW_{12}O_{40}^{3-}$ based PIL Janus nanosheets serve as a solid surfactant. A toluene-in-water emulsion forms. The $PW_{12}O_{40}^{3-}$ side can synchronously absorb methyl orange (MO) from water phase and catalytic degrade MO. The catalytic intermediate products are hydrophobic, which can be transferred to oil phase. The cooperative procedures can further facilitate the catalytic 40 degradation.

Herein, we report the synthesis of $PW_{12}O_{40}^{3-}$ based PIL Janus nanosheets and emulsion interfacial catalytic degradation of the example water soluble dye MO (Scheme 1). PIL functionalized Janus nanosheets are synthesized through a polymerization of an 45 ionic liquid monomer (ViEtIm$^+$Br$^-$) onto the ATRP agent terminated side of the Janus silica nanosheets. After a simple

anion exchanging Br$^-$ with $PW_{12}O_{40}^{3-}$, the $PW_{12}O_{40}^{3-}$ based PIL Janus nanosheets are derived. The Janus composite nanosheets are amphiphilic and can serve as a solid emulsifier to stabilize a 50 toluene-in-water emulsion. The example dye MO is preferentially absorbed within the PIL layer and degraded. The intermediate products are hydrophobic, which can transfer into the internal toluene oil phase. The transfer process can greatly facilitate further absorption and degradation. Higher degradation efficiency 55 is expected due to the cooperative interplay between the synchronous absorption, degradation and phase transfer.
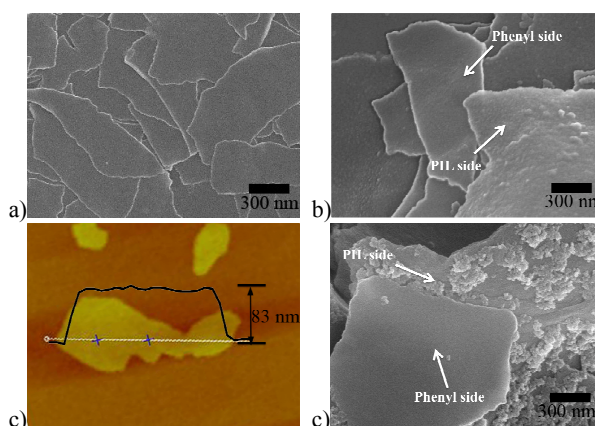

Figure 1. a) SEM image of the ATRP agent terminated Janus silica nanosheets; b, c) SEM and AFM images of the Br$^-$ based PIL Janus nanosheets; d) SEM image of the PIL Janus nanosheets after the PIL side is selectively labeled with the trisodium citrate capped Fe_3O_4 nanoparticles.

The phenyl/amine Janus silica nanosheets are obtained by self-65 organized sol-gel process at a Janus emulsion interface (Figure S1a). [10] They are thick ~58 nm (Figure S1b). An ATRP agent of 2-bromoisobutyryl bromide is selectively grafted onto the amine-group terminated side via amidation between (-COBr) and amine (-NH₂) groups. Both sides of the nanosheets remain smooth after 70 the ATRP agent grafting (Figure 1a). The nanosheets maintain thick ~58 nm. An ionic liquid monomer of 1-vinyl-3-ethylimidazolium bromide (ViEtIm$^+$Br$^-$) is polymerized from the ATRP agent grafted side of the nanosheets. Poly(ViEtIm$^+$Br$^-$)/silica composite Janus nanosheets are achieved (Figure 1b). The 75 PIL grafted side becomes slightly coarsening. The PIL Janus nanosheets become thicker ~83 nm (Figure 1c). Thermogravimetric analysis (TGA) indicates that the PIL content is 64 wt.-% (Figure S2). In order to prove the distinct compartmentalization of PIL on one side, negatively charged 80 citrate-capped Fe_3O_4 nanoparticles are used to selectively label the positively charged PIL (Figure 1d). The PIL side becomes more coarsening, while the other side maintains smooth. This

RSC Advances Accepted Manuscript

indicates that the other phenyl- group terminated side is not affected. The Br⁻ based PIL Janus nanosheets are well dispersible both in oil and water (Figure S3). This reveals that the nanosheets are amphiphilic.
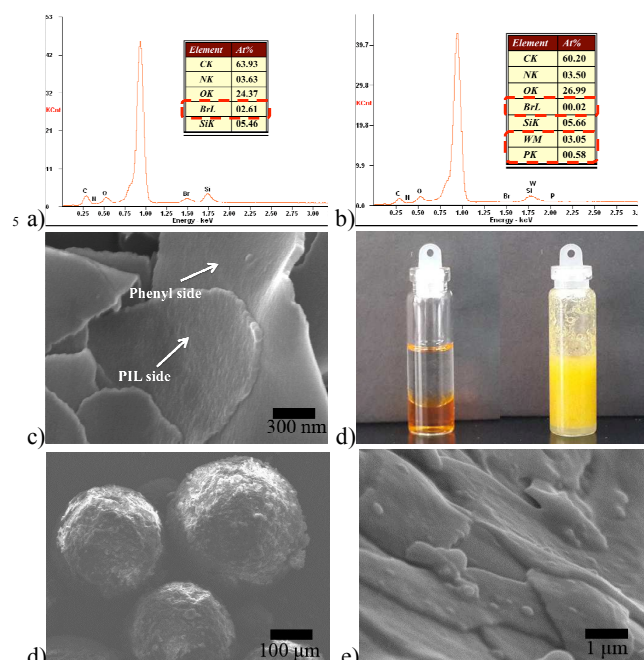

Figure 2. a) SEM image of the $PW_{12}O_{40}^{3-}$ based PIL Janus nanosheets; b) EDX spectra of the Br⁻ based PIL Janus nanosheets (1) and the $PW_{12}O_{40}^{3-}$ based PIL Janus nanosheets (2); c) immiscible toluene and water (left), and a toluene-in-water emulsion stabilized with the $PW_{12}O_{40}^{3-}$ based PIL Janus nanosheets, methyl orange is added to water as a chromogenic agent; d) SEM image of the paraffin droplets stabilized with the $PW_{12}O_{40}^{3-}$ based PIL Janus nanosheets; e) magnified SEM image of the paraffin droplet surface.

It is well known that anion type of PILs is broadly tunable by simple anion exchanging. $PW_{12}O_{40}^{3-}$ is introduced within the PIL layer through the anion exchange. The morphology is preserved (Figure 2c). 2.61 % of Br is measured from the Br⁻ based PIL Janus nanosheets (Figure 2a). After the anion exchange, the signal of Br almost disappear from the $PW_{12}O_{40}^{3-}$ based PIL Janus nanosheets (Figure 2b). 0.58 % of P and 2.05 % of W are measured. This indicates that Br⁻ has been completely exchanged with $PW_{12}O_{40}^{3-}$. The entire exchange has also been confirmed by XPS results (Figure S4) and FT-IR spectra (Figure S5). Presence of the imidazole cation is confirmed by the bands at 1700-1750 cm⁻¹. The bands at 800-1100 cm⁻¹ are assigned to $PW_{12}O_{40}^{3-}$. The $PW_{12}O_{40}^{3-}$ based PIL Janus nanosheets are well dispersible both in oil and water, indicating that the Janus performance is preserved (Figure S6). A toluene-in-water emulsion forms in the presence of the $PW_{12}O_{40}^{3-}$ based PIL Janus nanosheets (Figure 2d). In order to observe orientation of the PIL Janus nanosheets at the oil/water interface, melt paraffin (Tm: 52-54 °C) is employed to form a paraffin-in-water emulsion (Figure 2e). After the emulsion is cooled down to room temperature, the PIL Janus nanosheets are fixed at the emulsion interface. The coarsening PIL sides of all the nanosheets direct towards the aqueous continuous phase (Figure 2f).
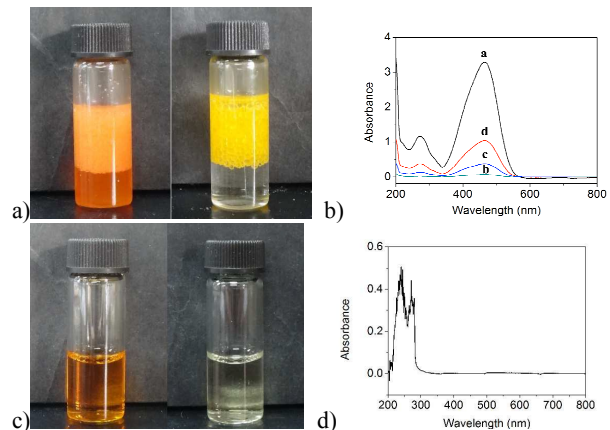

Figure 3. a) A toluene-in-water emulsion stabilized with the $PW_{12}O_{40}^{3-}$ based PIL Janus nanosheets (left); the emulsion after degradation in the presence of 10 μL H_2O_2 after 3 h (right); b) UV-vis spectra of 50 ppm MO aqueous solution (curve a), MO concentration in the aqueous phase after degradation by $PW_{12}O_{40}^{3-}$ based PIL Janus nanosheets in the oil-in-water emulsion (curve b), MO concentration after degradation by $PW_{12}O_{40}^{3-}$ based PIL Janus nanosheets in water phase (curve c), MO concentration after degradation by $PW_{12}O_{40}^{3-}$ based PIL Janus nanosheets in water phase but in the absence of H_2O_2 (curve d) c) MO aqueous solution (left) and after degradation (right) by $PW_{12}O_{40}^{3-}$ based PIL Janus nanosheets in water phase in the presence of 10 μL H_2O_2; d) UV-vis spectrum of the hydrophobic intermediate products extracted in toluene phase after the degradation.

$PW_{12}O_{40}^{3-}$ anion is highly effective heterogeneous catalyst to decompose organic dyes. [14,15] In our concern, water soluble MO is selected as a model organic dye. The intermediate products during degradation are oil soluble. [9] When the $PW_{12}O_{40}^{3-}$ based PIL Janus nanosheets are used as a solid emulsifier, toluene is emulsified in the water phase containing MO. Both the top emulsion and the bottom water phases are highly orange colorful (left Figure 3a). A given amount of H_2O_2 for example 10 μL is added to the emulsion to start the degradation at room temperature. After 3 h, the bottom water phase becomes colorless (right Figure 3a), and the top emulsion phase becomes yellow. The separated Janus nanosheets are yellow (Figure S7). This implies that some amount of MO has been absorbed by the Janus nanosheets. After washing with DMF, the yellow compound is confirmed to be MO by UV-vis spectroscopy. The absorption capacity is 12.7 wt.-% (Table 1). In the UV-vis spectra, the peak at 463 nm is characteristic of MO (curve a, Figure 3b). After 3 h, MO removal degree is high 99.2 wt.-% (curve b, Figure 3b). In comparison, the removal becomes lower (Figure 3c) when the $PW_{12}O_{40}^{3-}$ based PIL Janus nanosheets are present in water phase (curve c, Figure 3b). 88.4 wt.-% removal is achieved. MO absorption capacity is 8.1 wt.-% (Table 1). Since MO can be easily extracted by ionic liquids, it is understandable that MO is preferentially adsorbed within the $PW_{12}O_{40}^{3-}$ based PIL side of the Janus nanosheets. H_2O_2 is crucial for the oxidative degradation. H_2O_2 can induce $PW_{12}O_{40}^{3-}$ to form more active peroxides such as $[(PO_4)\{WO(O_2)_2\}_2\{WO(O_2)_2(H_2O)\}]^{3-}$ and $[(PO_4)\{WO(O_2)_2\}_4]^{3-}$. [14] In comparison, in the absence of H_2O_2 (Figure S8), 69.2 wt-% removal is achieved (curve d, Figure 3b). MO absorption capacity is 42.8 wt.-% (Table 1). At low feeding levels below 5 μL, both the degradation degree and rate increase with the amount of H_2O_2. At high feeding levels, the degradation efficiency is less influenced by further increasing H_2O_2 feeding for example from 10 μL to 15 μL. This is understandable that 10

μL of H_2O_2 is sufficient to activate all the $PW_{12}O_{40}^{3-}$ groups. Therefore, the feeding amount of H_2O_2 is fixed at 10 μL in the current work. After a prolonged reaction time for example one week, the top yellow emulsion phase becomes colorless (Figure

5 S9). The absorbed MO diffuses slowly and can be degraded eventually. In the emulsion interfacial catalysis, the hydrophobic intermediate products after degradation can be transferred in the oil phase, which can greatly enhance the degradation efficiency. The intermediate products as shown in the Scheme have been

10 separated from toluene phase, which are confirmed by new peaks in the UV-vis spectrum (Figure 3d). Ionic liquid functionalized Janus nanosheets reported in our previous research [13] also could degrade the MO in similar emulsion system. The degradation efficiency is only 52.0 %, which is far lower than the PIL Janus

15 nanosheets due to the amount of $PW_{12}O_{40}^{3-}$ ions decreases substantially.

Method	MO absorption (wt.-%)	Total MO removal (wt.-%)
emulsion system	12.7	99.2
water phase	8.1	88.4
water phase (without H_2O_2)	42.8	69.2

Table 1. Degradation and absorption of MO by the two methods of emulsion system and water phase. T=25 °C, V_{MO}= 2 mL, $m_{catalyst}$ = 5 mg, 10 μL of H_2O_2.
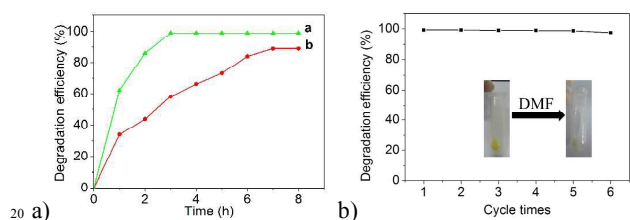

20 a)   b)

Figure 4. a) Degradation kinetics of MO by emulsion system (a) and water phase (b); b) catalyst recycling of the PIL Janus nanosheets in the emulsion method.

25 Besides degradation degree, degradation kinetics is another concern. Degradation is very fast at early stage in the emulsion method. After 3 h, degradation comes to nearly completion of 99.2%. In contrast, in water phase the degradation occurs slower and proceeds gradually even after 6 h. The PIL based Janus

30 nanosheets can be easily regenerated by centrifugation and washing with DMF. After washing to remove the absorbed MO dye, 100% activity is preserved after 6 recycling (Figure 4b).

In summary, $PW_{12}O_{40}^{3-}$ based PIL Janus nanosheets are synthesized by ATRP of IL monomer onto the hydrophilic side of

35 the silica Janus nanosheets following by an anion exchange. At an oil/water emulsion interface, the Janus nanosheets demonstrate higher degradation of the example water soluble dye MO. They can be completely regenerated. The PIL Janus nanosheets should be promising in heterogeneous decomposition of water soluble

40 dyes.

Acknowledgement

Notes and references

45 [a]*Liaoning Key Laboratory for Green Synthesis and Preparative Chemistry of Advanced Materials, College of Chemistry, Liaoning University, Shenyang 110036, China. Fax: 8624-62202380; Tel: 8624-62202378; E-mail: songlab@lnu.edu.cn (X.M.S).*
[b]*State Key Laboratory of Polymer Physics and Chemistry, Institute of*
50 *Chemistry, Chinese Academy of Sciences ,Beijing 100190, China. Fax: 8610-62559373; Tel: 8610-82619206; E-mail: liangfuxin@iccas.ac.cn (F.L).*
† Electronic Supplementary Information (ESI) available: Experimental section and supplimental figures. See DOI: 10.1039/b000000x/

55

[1] O. Legrini, E. Oliveros, A. M. Braun, *Chem. Rev.* **1993**, 93, 671.

[2] M. R. Hoffmann, S. T. Martin, W. Choi, D. W. Bahnemannt, *Chem. Rev.* **1995**, 95, 69.

[3] I. M. Arabatzisa, T. Stergiopoulosa, D. Andreevab, S. Kitovac, S. G.
60 Neophytidesd, P. Falarasa, *J. Catal.* **2003**, 220, 127.

[4] G. Annadurai, R. S. Juang, D. J. Lee, *J. Hazard. Mater.* **2002**, 92, 263.

[5] C. T. M. J. Frijtersa, R. H. Vos, G. Schefferb, R. Muldera, *Water Res.* **2006**, 40, 1249.

[6] C. Ritchie, C. Streb, J. Thiel, S. G. Mitchell, H. N. Miras, D. L. Long, T.
65 Boyd, R. D. Peacock, T. McGlone, L. Cronin, *Angew. Chem. Int. Ed.* **2008**, 47, 6881.

[7] R. Liu, S. Li, X. Yu, G. Zhang, S. Zhang, J. Yao, B Keita, L. Nadjo, L. Zhi, *Small* **2012**, 8, 1398.

[8] Y. Guo, Y. Wang, C. Hu, Y. Wang, E. Wang, *Chem. Mater.* **2000,** *12,* 3501.
70 [9] C. Galindo, P. Jacques, A. Kalt, *J. Photoch. Photobio. A* **2000**, 130, 35.

[10] F. X. Liang, K. Shen, X. Z. Qu, C. L. Zhang, Q. Wang, J. L. Li, J. G. Liu, Z. Z. Yang, *Angew. Chem. Int. Ed.,* **2011**, 50, 2379.

[11] Y. Chen, F. X. Liang, H. L. Yang, C. L. Zhang, Q. Wang, X. Z. Qu, J. L. Li, Y. L. Cai, D. Qiu, Z. Z. Yang, *Macromolecules* **2012**, 45, 1460.
75 [12] H. L. Yang, F. X. Liang, X. Wang, Y. Chen, C. L. Zhang, Q. Wang, X. Z. Qu, J. L. Li, D. C. Wu, Z. Z. Yang, *Macromolecules* **2013**, 46, 2754.

[13] X. Y. Ji, Q. Zhang, F. X. Liang, Q. Chen, X. Z. Qu, C. L. Zhang, Q. Wang, J. L. Li, X. M. Song, Z. Z. Yang, *Chem. Commun.* **2014**, 50, 5706.

[14] D. C. Duncan, R. C. Chambers, E. Hecht, C. L. Hill, *J. Am. Chem. Soc.*
80 **1995**, 117, 681.

[15] A. Dolbecq, P. Mialane, B. Keita, L. Nadjo, *J. Mater. Chem.* **2012**, 22, 24509.

RSC Advances Accepted Manuscript